Wave Packet Incident on Negative-Index Media

John Rhodes Thomas, *Member, IEEE,* and Akira Ishimaru, *Life Fellow, IEEE*

***Abstract*—This paper presents a study of the refraction and reflection of a wave packet in time and space at the plane boundary between free space and a negative index medium (NIM). We derive an analytic asymptotic expression that shows negative refraction at the angle predicted by the negative index evaluated at the center frequency with a speed of propagation in the NIM equal to the group velocity. Then we present numerical calculations of exact solutions that verify the asymptotic theory. Finally we present numerical calculations for cases with incidence beyond the critical angle. Here we find phenomena identified as backward lateral waves and a negative Goos–Hanchen shift.**

***Index Terms*—Beam wave, lateral wave, negative refraction, reflection, surface wave, transient propagation.**

I. Introduction

MATERIAL with negative refractive index was first proposed by Veselago in 1968 [1] and recently it has attracted considerable attention through the work of Pendry, Smith and others [2]–[4]. This medium has been called negative index medium (NIM) [5], or left-handed medium (LHM), or double negative medium (DNG) [6]. When a plane wave is incident on NIM, the wave is refracted negatively according to Snell's law. It has also been shown that the group front of a plane wave refracts positively, but a modulated Gaussian beam refracts negatively. In this work we use a space-time domain approach to clarify the refraction, causal requirements, and dispersion that apply to a space-time beam wave packet. In so doing we discuss the refraction of a beam packet for cases when the incident angle is less or greater than the critical angle. This approach leads to a study of the Goos–Hanchen effect and to confirmation of a new wave, the "backward lateral wave," which we predicted in a recently submitted paper [7].

We study the propagation of a space-time wave packet (a pulsed beam wave) that has nearly planar properties near the middle of the beam and nearly cw properties near the mid-point in time of the pulse. We treat here a 2-D Gaussian beam wave modulated with a Gaussian time dependence. In free space this wave packet has negligible change in cross section or time-domain envelope for distances such that $\lambda_o z' \ll \pi W_o^2$ where λ_o is the wavelength at the central frequency of the pulse, z' is distance along the direction of propagation of the central direction of the beam, and W_o is the beam cross section. For example, if $W_o = 10\lambda_o$, then the beam wave will retain its coherence for several 10's of wavelengths. We will show that this packet, incident on a planar boundary of a NIM, exhibits negative refraction plus a skewing and distortion of the elliptical cross section of the incident pulse. The skewing effect is due to the positive refraction of what we call the wavefront normal, but which is also identified as the interference front normal by Smith *et al.* [8]. We have obtained an analytic first-order asymptotic approximation that shows the roles of the group velocity, the phase velocity and the wave fronts of the beam. From this expression, we find that the center of the wave packet refracts negatively according to Snell's law and propagates with the group velocity. However, the wave normal, which is a vector normal to the wave front, refracts positively and propagates with a velocity different from the group velocity. We will use a p-polarized wave packet, but the results apply equally to the s-polarized packet.

We have implemented numerical calculations to confirm the approximations and to show smaller second-order effects. This numerical calculation has also been applied to a case for which we predicted the existence of a backward lateral wave. The backward lateral wave occurs in a NIM when the angle of incidence is beyond the critical angle. With incidence from free space on a lossless NIM, existence of a critical angle [7] requires $-1 < n < 0$.

Manuscript received July 20, 2004. This work was supported by the National Science Foundation under Grant ESC-9908849.

The authors are with the Department of Electrical Engineering, University of Washington, Seattle, WA 98195 USA (e-mail: ishimaru@ee.washington.edu).

Digital Object Identifier 10.1109/TAP.2005.846454

II. Analytical Formulation

We consider the interface between a half space of a NIM and free space, with the normal direction to the boundary plane being the Z direction, positive into the NIM. The incident wave packet is taken as p-polarized, completely determined by one component of the magnetic field, which we take to be in the Y direction. The incident wave packet in free space (E_x, E_z, H_y) is then given by $H_y(x,z,t) = \mathrm{Re}\{\psi_i(x,z,t)\}$ with

$$\psi_i = \exp\left[j\omega_o\left(t - \frac{z'}{c}\right) - \frac{\left(t - \frac{z'}{c}\right)^2}{T_o^2} - \frac{x'^2}{W_o^2}\right] \quad (1)$$

where ω_o = carrier frequency, c = speed of light, $T_o = 2/\Delta\omega$, $\Delta\omega$ = frequency band, and W_o is the full width of the packet at $1/e$ of its peak amplitude in the x' direction. As shown in Fig. 1, the incident packet propagates along the z' coordinate, and x' is the transverse coordinate of the packet. The (x', z') coordinates are related to (x, z) through rotation by the angle of incidence θ_o of the beam centerline. The electric field is obtained as $\vec{E} = (1/(j\omega\epsilon_o))\nabla \times (H_y\hat{y})$. This is a collimated wave packet applicable when $W_o \gg \lambda_o$ and $\Delta\omega \ll \omega_o$. To obtain the analytical expression for the packet in the medium, we first rotate the coordinate system from (x', z') to (x, z) and take a double Fourier transform with respect to direction x and time t at $z = 0$.

$$\begin{aligned}\bar{\psi}_i(k_x, 0, \omega) &= \int_{-\infty}^{\infty}\int_{-\infty}^{\infty} \psi_i(x,z,t)\exp(-j\omega t + jk_x x)dtdx \\ &= \frac{\pi W_o T_o}{\cos\theta_o}\exp\left[-\frac{(\omega-\omega_o)^2 T_o^2}{4}\right. \\ &\qquad \left. -\frac{\left(k_x - \frac{\omega}{c}\sin\theta_o\right)^2 W_o^2}{4\cos^2\theta_o}\right]. \quad (2)\end{aligned}$$

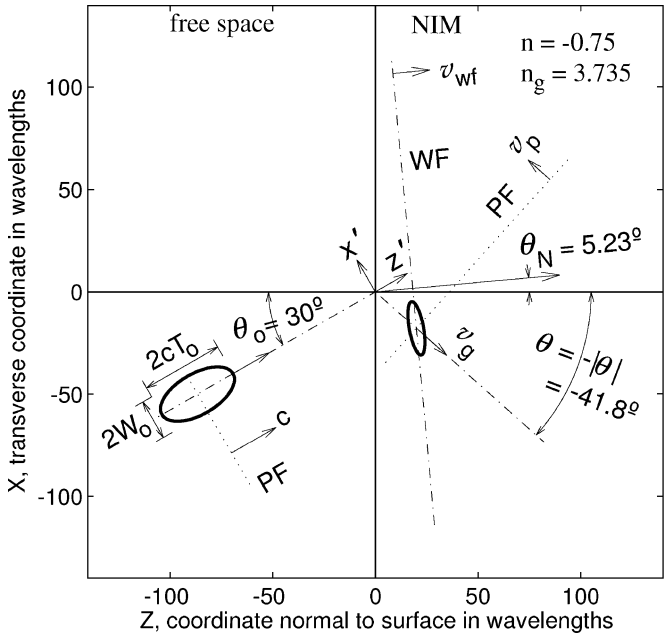

Fig. 1. Wave packet incident on negative refractive index medium. Wave packets are shown as heavy contour lines of $|H|$ at a level of 1/e from the peak. The incident packet is shown at time $-5T_o$ and the refracted packet at time $5T_o$ relative to time of incidence of the peak. The wave packet propagates with the group velocity v_g in the direction $\theta = -|\theta|$. The wave front (WF) propagates with the wavefront velocity v_{wf} in the direction of the wave normal $\mathbf{N}(\theta_N)$. The phase front (PF) propagates with the phase velocity v_p in the direction opposite to the group velocity.

To obtain the field in the NIM where $z > 0$ (medium 2), we multiply by the transmission coefficient $T(k_x, \omega)$ and the propagation factor $\exp(-jk_{z2}z)$, and then take the inverse Fourier transform. We obtain

$$\psi_t(x,z,t) = \frac{1}{(2\pi)^2}\int_{-\infty}^{\infty}\int_{-\infty}^{\infty}\left[T(k_x,\omega)\bar{\psi}_i(k_x,0,\omega) \times \exp(-jk_{z2}z - jk_x x + j\omega t)dk_x d\omega\right] \quad (3)$$

where

$$T(k_x,\omega) = \frac{\frac{2k_{zi}}{\epsilon_o}}{\left(\frac{k_{zi}}{\epsilon_o}\right) + \left(\frac{k_{z2}}{\epsilon}\right)}$$

$$k_{zi} = \sqrt{k^2 - k_x^2}, \quad k_{z2} = \sqrt{(kn)^2 - k_x^2}, \quad k = \frac{\omega}{c}.$$

In the computation of k_{zi} and k_{z2}, care must be taken to choose the square root which corresponds to attenuation of the outgoing wave; that is a negative imaginary part for the $\exp(+j\omega t)$ convention used here. Similarly the reflected wave is obtained by multiplying by the reflection coefficient $R(k_x, \omega)$ and a propagation factor $\exp(+jk_{zi}z)$ for a negative-going wave in the free-space medium. Thus, in the time domain

$$\psi_r(x,z,t) = \frac{1}{(2\pi)^2}\int\int\left[R(k_x,\omega)\bar{\psi}_i(k_x,0,\omega) \times \exp(+jk_{zi}z - jk_x x + j\omega t)dk_x d\omega\right]. \quad (4)$$

Assuming that $T(k_x, \omega)$ is a slowly varying function of k_x and ω, we can evaluate (3) by an approximation method that is essentially an application of the method of steepest descent. The approximation is asymptotic in the large parameters W_o and T_o. Noting that $\bar{\psi}_i$ in (2) is highly peaked near ω_o and $(\omega_o/c)\sin\theta_o$, we expand k_{z2} and keep the first-order terms

$$k_{z2} = k_{zo} + k_x'\frac{\partial k_{z2}}{\partial k_x} + \omega'\frac{\partial k_{z2}}{\partial \omega} \quad (5)$$

where $k_x' = k_x - (\omega_o/c)\sin\theta_o$, $\omega' = \omega - \omega_o$, and $\partial k_{z2}/\partial k_x$ and $\partial k_{z2}/\partial\omega$ are evaluated at ω_o and $k_{xo} = (\omega_o/c)\sin\theta_o$. With $T(k_x,\omega) = T(k_{xo},\omega_o)$ the inner integral on k_x is a straight-forward example of completing the square in (k_x—linear shift term) and finding the remaining term that is independent of k_x times a known definite integral that gives a factor of $2\sqrt{\pi}\cos(\theta_o)/W_o$. Then, the outer integral on ω can be done by the same method. This second integral has many terms, and requires considerable manipulation to reduce it to obtain this final analytical expression for $\psi_t(x,z,t)$.

$$\begin{aligned}\psi_t(x,z,t) &= T(k_{xo},\omega_o)e^{-j\phi}F_bF_a\\ \phi &= k_{zo}z + k_{xo}x - \omega_o t\\ F_b &= \exp\left[-\left(x + \frac{\partial k_z}{\partial k_x}z\right)^2\frac{\cos^2\theta_o}{W_o^2}\right]\\ F_a &= \exp\left[-\frac{(t - \vec{N}\cdot\vec{r})^2}{T_o^2}\right]\end{aligned} \quad (6)$$

where the vector $\vec{N}$ is defined as

$$\vec{N} = \frac{\sin\theta_o}{c}\hat{x} + \frac{1}{c}\frac{(nn_g - \sin^2\theta_o)}{\sqrt{n^2 - \sin^2\theta_o}}\hat{z}$$

and the other subsidiary quantities are

$$\begin{aligned}k_{xo} &= \frac{\omega_o}{c}\sin\theta_o = \frac{\omega_o}{c}n\sin\theta_2, \quad k_o = \frac{\omega_o}{c}\\ k_{zo} &= \sqrt{k_o^2n^2 - k_{xo}^2} = k_o\sqrt{n^2 - \sin^2\theta_o} = k_o n\cos\theta_2\\ \frac{\partial k_z}{\partial k_x} &= -\frac{k_{xo}}{k_{zo}} = -\tan\theta_2\\ n_g &= \text{group refractive index} = \frac{\partial(\omega n)}{\partial\omega}.\end{aligned} \quad (7)$$

Derivation of the group refractive index in (7) has been presented by many classic authors including Brillouin [9] and Born and Wolf [10]. From the equations following (6) until Section III we will use short notation that $n = n(\omega_o)$ and

$$n(\omega) = n + \frac{(n_g - n)\omega'}{\omega_o}. \quad (8)$$

This first-order approximation is used in the analytic asymptotic approximation and also later in what we call the linear model.

The angle θ_2 is the angle of refraction given by Snell's law for incidence at the central angle θ_o of the packet. The indexes n and n_g as well as $\partial k_z/\partial k_x$ are to be evaluated at ω_o and k_{xo}. The square root choice for k_{zo} is now well understood. It is plus or minus for n plus or minus, respectively. More rigorously, it is chosen so that $\mathrm{Im}\{k_{zo}\} < 0$ and that $\mathrm{Im}\{\epsilon\} < 0$ and $\mathrm{Im}\{\mu\} < 0$. Also note that since n is negative, the phase velocity $v_p = c/n$ is negative. However, the group refractive index n_g and the group velocity v_g are positive. These are consistent with Smith *et al.* [8].

We note that this approximation applies when the transmitted wave is not evanescent, that is when there is no critical angle for total reflection or when the incident angle is not greater than

this critical angle. We shall return to incidence at angles beyond the critical angle in Section IV.

The equation for the reflected field can be evaluated by the same method as described for the transmitted wave. If one makes only the approximation that $R(k_x,\omega) = R(k_{xo},\omega_o)$, the resulting reflected field is the specular reflection of the incident wave with all frequency components having this central reflection coefficient. Thus, that approximation would correspond to a beam wave propagating coherently for distances small compared to $\pi W_o^2/\lambda_o$ and then showing dispersion. However, if the further approximation is made as to $k_{zi} = \sqrt{k_{zo}^2 - k_x^2}$, then the elliptical beam cross section will just move uniformly outwards at the specular reflection angle with speed of light c.

Equation (6) and the following definitions show three features of wave propagation in the NIM due to the product of three functions. (1) The phase term $\exp(-j\phi) = \exp(-jnk_o[\cos\theta_2 z + \sin\theta_2 x - (c/n)t])$ shows phase progression according to Snell's law with $n\sin\theta_2 = \sin\theta_o$. Thus, the angle of refraction θ_2 and the phase velocity are negative because the index of refraction is negative. (2) The factor F_b clearly shows that the peak of the transmitted packet follows the line $x = z\tan\theta_2$. That is, the energy associated with the E and H fields of the packet is refracted negatively. (3) The factor F_a exhibits planar fronts given by

$$t - \vec{N}\cdot\vec{r} = \text{constant} \tag{9}$$

The transmitted packet's skewed oval amplitude contour results from the product of the factors F_b and F_a. The vector $\vec{N}$ is in the direction of the normal to the fronts of F_a. In connection with analysis of a modulated plane wave these fronts have been called interference fronts by other authors [8], [11] and also group fronts [12]. The angle θ_N between the vector $\vec{N}$ and the Z-axis is given by (Fig. 1)

$$\tan\theta_N = \frac{N_z}{N_x} = \frac{\sin\theta_o\sqrt{n^2 - \sin^2\theta_o}}{nn_g - \sin^2\theta_o}. \tag{10}$$

Here, we need to choose the correct sign for the square root, which comes from the occurrence of $k_{z2o} = k_o\sqrt{n^2 - \sin^2\theta_o}$. This propagation factor must have a negative imaginary part for attenuation of the outward going wave. To have transmission into the NIM and not total reflection, we must have $n^2 > \sin^2\theta_o$. For completeness we now consider the cases of both positive and negative index. For positive n the square root must be positive in its dominant real part, and we expect the group velocity to be smaller than the phase velocity, so $n_g > n$. Thus, the numerator and denominator of the fraction in (10) are positive and θ_N is positive. For negative n, k_{z2o} and the square root must be negative in its (dominant) real part. Since the group index must be positive and greater than 1 for causal signal propagation [9], the fraction on the right of (10) is positive and again θ_N is positive.

Fig. 1 illustrates these asymptotic-approximation results for a case with $n = -0.75$ and $n_g = 3.735$. These index values are chosen in a somewhat arbitrary way. We have chosen to study negative indexes somewhere near -1. With the choice of $n = -0.75$, the group index of 3.735 corresponds to that of a Drude–Lorentz model discussed below. The angle of incidence is chosen as 30°, well below the critical angle of approximately 48.6°. The beam wave packet of (1) is chosen to have a transverse half-width $W_o = 10\lambda_o$ and a half-length along the direction of propagation of $cT_o = 20\lambda_o$. The width and length are taken to the $1/e$ amplitude relative to the peak, and this choice of T_o amounts to a bandwidth Δf to the $1/e$ amplitude in frequency $\Delta f/f_o = 0.05\pi$. This is a reasonably narrow bandwidth and the choice of n_g as a constant across the integral in (4) is a reasonable approximation. Any material (metamaterial) with negative index of refraction will have strong dispersion. Variations with frequency may be modeled with a Drude (plasmonic) model [13], a Drude–Lorentz model, or possibly a still more complex model. However, a Drude–Lorentz model, also referred to as a Lorentz model or Lorentz medium, provides what we may call a physical model with 3 parameters for permittivity. As also considered by [6], we shall use the same form to characterize the negative permeability. In the next section we shall consider cases that correspond to a Lorentz model, and carry out numerical solutions of the exact integral equations (3) and (4) for a single-resonance Drude–Lorentz behavior of both permittivity and permeability. To show the generality of the approach, ϵ and μ are taken to be somewhat different.

The term Drude–Lorentz (or Lorentz) model refers to a classical model for electrons, bound with a simple-harmonic-oscillator potential, interacting with a cw electromagnetic field. The relative permittivity of such a medium has the form

$$\epsilon_r = 1 + \frac{\omega_{pe}^2}{\omega_e^2 - \omega^2 + j\omega\Gamma_e} \tag{11}$$

where ω_{pe} is the plasma frequency of the electrons, ω_e is the harmonic oscillator frequency, and Γ_e the collision frequency. In the low-loss case $\Gamma_e \ll \omega_{pe}$. We also use this frequency variation with assigned parameters for the relative permeability μ_r. For the low-loss case the real part of (11) has a negative minimum at a frequency slightly above ω_e given by $\omega^2 = \omega_e(\omega_e + \Gamma_e)$. This minimum is

$$\min\left(\text{real}(\epsilon_r)\right) = 1 - \frac{\omega_{pe}^2}{2\omega_e\Gamma_e + \Gamma_e^2} \approx 1 - \frac{\omega_{pe}}{2\omega_e}\frac{\omega_{pe}}{\Gamma_e}.$$

Since $\omega_{pe} \gg \Gamma_e$ and ω_e is typically of the same order as ω_{pe}, it is possible to set ϵ_r equal to any reasonable negative value at some frequency in the normal dispersion region slightly above this minimum.

III. Numerical Solutions: Cases Without a Critical Angle θ_c or With Angle of Incidence Less Than θ_c

We have calculated solutions to (3) and (4) with brute-force numerical integrations. The standard computations are based on a grid of 2066 values of k_x by 1811 values of ω. It is a variable-step grid with finer steps near the central peak of the Gaussian and coarser steps out toward the edge of the rectangular integration area. The integration method is trapezoidal. We note that (3) and (4) could be considered as scaling in frequency relative to center frequency ω_o and x component of wavenumber relative to the center $k_{xo} = (\omega_o/c)\sin\theta_o = k_o\sin\theta_o$ if

- the Gaussian widths are expressed in wavelengths, that is $W_o = W_n\lambda_o$ and $cT_o = T_n\lambda_o$ with $\lambda_o = 2\pi/k_o$ and the subscript n denoting normalized;
- the permittivity and index of refraction are scaled as functions of frequency relative to this normalized frequency.

This result essentially follows from the electrodynamic similitude of Maxwell's equations [14]. We carried out computations for a specific center frequency $f_o = 10^{11}$ Hz, but we show results plotted in wavelength units for x and z, which would then apply to any center frequency so long as the index of refraction and permittivity are scaled correspondingly.

We consistently computed cases with $W_o = 10\lambda_o$ and $cT_o = 20\lambda_o$ as in Fig. 1. With these fairly rapid Gaussian cutoffs, we found that we could obtain good results with a grid where $(k_x - k_{xo})W_o/(2\cos\theta_o)$ extends from -14 to $+16$ and where $(\omega - \omega_o)T_o/2$ extends from -13 to $+13$. These choices make the Gaussian factors become $\exp(-14^2) \approx 7.6 \cdot 10^{-86}$, $\exp(-16^2) \approx 6.6 \cdot 10^{-112}$, and $\exp(-13^2) \approx 4.0 \cdot 10^{-74}$ on the outer edges along the center lines of the other variable, respectively. We found these limits and the grid fineness by trial and error where we required that the main parts of the transmitted and reflected fields change by less than 1 part in 10^6 as we went to a next test with larger limits or finer grids.

We limited our computations to times such that $ct < 10\lambda_o$, where $t = 0$ is the time when the incident pulse is centered at the origin, per (1). Hence, the maximum values of x and z where the pulse is of interest in the cases we examined is limited to about $200\lambda_o$. Finer grids would be required for larger values of x and z. Also, a finer grid is required for some small-amplitude fields considered in the last section on backward lateral waves.

We present a selection of cases to illustrate the following features of reflection from and refraction in a NIM.

- The asymptotic approximation gives a very accurate description of the motion of the peak of the transmitted wave. The peak follows the line at the Snell's law angle of the center frequency, and it moves with the speed of the group velocity of the center frequency. The peak amplitudes are fairly close to the approximate prediction.
- The elliptical amplitude distribution is skewed and rotated in coarse agreement with the asymptotic approximation. The size of the contour at 1/e of the peak is quite close to that predicted by the asymptotic approximation.
- As expected, the reflected wave is well predicted by specular reflection of the pulse with the reflection coefficient of the center frequency.
- The curved variation of index of refraction in a Lorentz model provides some asymmetry to the transmitted pulse, but still leads to a pulse that reasonably follows the asymptotic approximation.

Figs. 2 and 3 show comparisons of numerical solutions to the exact Fourier integral equations (3) and (4) for cases corresponding to the asymptotic solution shown in Fig. 1. Because the reflection and transmission coefficients R and T depend on ϵ_{2r} as well as n_{2r}, it is necessary to specify this additional quantity at the band center as well as functions to determined their variation across the frequency band of integration. We chose a band-center value $\epsilon_{2ro} = -0.8 - 0.002j$. Then, the band-center value of relative permeability is $\mu_{2ro} = n_{2o}^2/\epsilon_{2ro} = -0.703\,12 - 0.000\,117j$. To specify the variation of n and ϵ across the band we consider two cases. They are: (a) a single-resonance Lorentz model for ϵ_{2r} and μ_{2r} and (b) a linear model for ϵ_{2r} and n_2. We include just one linear model calculation. It shows that the transmitted pulse in the NIM is relatively insensitive to details of the variation of n and ϵ_r about the center frequency if the relatively wide-band condition applies.

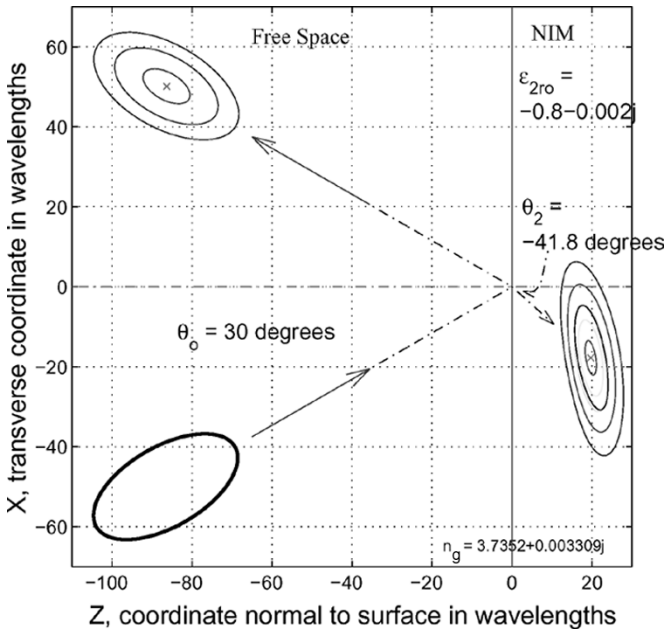

Fig. 2. Contour plots of $|H|$ for Lorentz model with $n_{2o} = -0.75 - 0.001j$ at $\text{time} = 5T_o$ for transmitted and reflected fields. The incident contour is at $\text{time} = -5T_o$. From exact theory numerical field calculations, the transmitted contours are at levels of 0.9, 0.6, 1/e, $0.4 * 1/e$, and $0.1 * 1/e$ relative to the peak of 0.8855 and reflected contours at 0.9, 0.6, and 1/e relative to this peak of 0.1085. For the analytic asymptotic approximation only the 1/e contours of the incident and transmitted wave are shown (in black). ($\text{Incident peak} = 1.0$, $\text{transmitted peak} = 0.9358$.)

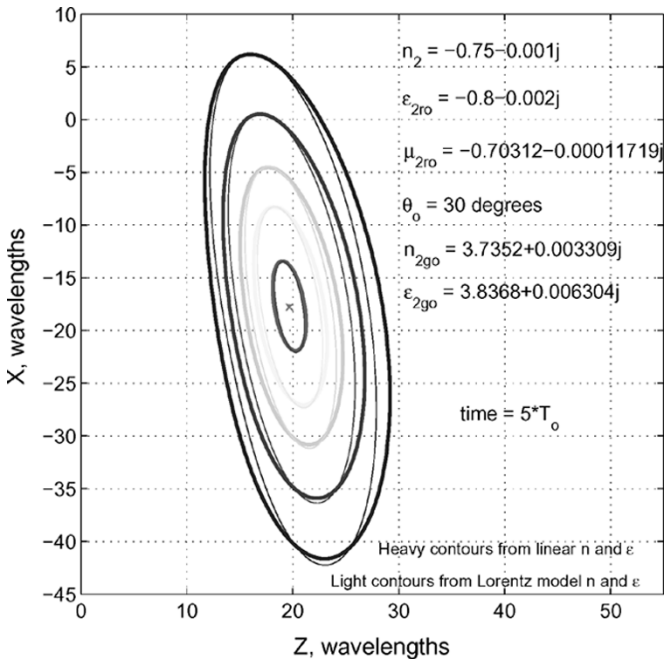

Fig. 3. Close comparison of transmitted (refracted) pulses. Comparison is of Lorentz model variation of n_2 and ϵ_{2r} versus a model with linear variation of n_2 and ϵ_{2r} with matching n_g and e_{2rg} at central frequency. Contour levels are 0.9, 0.6, 1/e, $0.4 * 1/e$, $0.1 * 1/e$ relative to the respective peaks.

We have chosen a single-resonance Lorentz model for several reasons. It has only 3 parameters for the permittivity and another 3 for the permeability. Also, the Lorentz model has been considered as a simple physical example by several other researchers in the study of NIM, e.g., [6], [8]. Two of the three conditions to determine these parameters are set by the choice of real and imaginary parts of ϵ_{2ro} and n_{2o} (which determine μ_{2ro}). The third condition we shall take arbitrarily is a moderately wide-band condition.

Thus, we take $\epsilon_r(\omega)$ as given by (11). The analogous Lorentz form of the permeability is taken as

$$\mu_r = 1 + \frac{\omega_{pm}^2}{\omega_m^2 - \omega^2 + j\omega\Gamma_m}. \tag{12}$$

We have chosen a wide-band condition $\omega_{pe}/\omega_e = \omega_{pm}/\omega_m = 2.5$. The larger the choice of this ratio, the wider the band of the resonance. The limit of this ratio approaching infinity leads to a pure Drude (plasma) model.

The group index at frequency ω_o is given by

$$n_g = \frac{n(\omega_o)}{2}\left[\frac{1}{\epsilon_r}\frac{\partial(\omega\epsilon_r)}{\partial\omega} + \frac{1}{\mu_r}\frac{\partial(\omega\mu_r)}{\partial\omega}\right] = \frac{n(\omega_o)}{2}\left[\frac{\epsilon_{rg}}{\epsilon_r} + \frac{\mu_{rg}}{\mu_r}\right] \tag{13}$$

where the term in square brackets is evaluated at ω_o. We define the group relative permittivity by analogy as $\epsilon_{rg} = \partial(\omega\epsilon_r)/\partial\omega$ and similarly for permeability. In the linear model, the group index matches the slope of $n(\omega)$ at ω_o. For our case of $n_{2o} = -0.75 - 0.001j$, $\epsilon_{2r} = -0.8 - 0.002j$, $\mu_{2r} = n_2^2/\epsilon_{2r}$ and the wide-band condition as stated, then $n_g = 3.7352 + 0.003\,309j$. The linear model also requires the value of the linear fit to ϵ_{2r} at $\omega = \omega_o$ given by ϵ_{2rg}, which from (11) and (13) is

$$\epsilon_{2rg} = \epsilon_{2ro}\left[1 + \frac{\omega_o\omega_{pe}^2(2\omega_o - j\Gamma_e)}{(\omega_e^2 - \omega_o^2 - j\omega_o\Gamma_e)^2\,\epsilon_{2ro}}\right] = 3.8368 + 0.006\,304j. \tag{14}$$

The Lorentz model gives a positive imaginary part for ϵ_{2rg} and n_g. This is evident from classic Lorentz model dispersion curves-in the normal dispersion region above the resonant frequency, the magnitude of the imaginary part of $\epsilon(\omega)$ is decreasing. However, this result will not violate the outgoing radiation condition within our band of approximation. In this band $n(\omega)$ is given by (8) and $\epsilon(\omega) = \epsilon(\omega_o) + (\epsilon_{2rg} - \epsilon(\omega_o))(\omega - \omega_o)/\omega_o$. If $\mathrm{Im}\{\epsilon\} = \epsilon''$ and $\epsilon''(\omega_o) = -\Delta_1$ where $-\Delta_1$ is a small positive quantity, then $\epsilon''_{2rg} = \Delta_2$ where Δ_2 is a positive quantity of the order of Δ_1 and

$$\epsilon'' = -\Delta_1 + \frac{(\Delta_2 + \Delta_1)(\omega - \omega_o)}{\omega_o} < 0 \tag{15}$$

within our band of integration. In other words, (15) shows that even though the $\mathrm{Im}\{\epsilon_{rg}\}$ is positive, $\mathrm{Im}\{\epsilon\}$ is negative. The same reasoning applies to $\mathrm{Im}\{n\}$.

Fig. 2 shows the numerically calculated contours of the magnitude of the transmitted field and reflected field at a time $t = 5T_o$ as in Fig. 1. Fig. 2 also shows black contours at 1/e of the peak for the incident wave at time $t = -5T_o$ and for the asymptotic approximation for the transmitted wave at $5T_o$. The third numerical contour at 1/e of the transmitted peak is very close to the black 1/e contour from the analytic approximation. This illustrates that the asymptotic approximation works well for the Lorentz model with incidence not beyond the critical angle. We want to emphasize this point since the asymptotic approximation utilizes only the linear variation as given by (13) and is given analytically by (6) and (7).

There are several significant points concerning these calculations.

- The peak of the numerical integral calculation for the transmitted wave follows very closely along the Snell's angle line at the group velocity. The "x" in Fig. 2 at the location of the transmitted peak has coordinates $x/\lambda_o = -17.67$ and $z/\lambda_o = 19.65$. The asymptotic approximation has its peak at $X_p/\lambda_o = (5cT_o/n_g)\sin\theta_2 = -17.85$ and $Z_p\lambda_o = (5cT_o/n_g)\cos\theta_2 = 19.95$. With an incident peak normalized to 1, the amplitude of the peak from numerical integration is 0.831, as compared to the asymptotic approximation value of 0.936. In general, we find the magnitude of the transmitted asymptotic peak to agree only within about 10% of the result found by numerical integration. The numerical integration depends on the value and variation of the relative permittivity ϵ_{2r}, whereas the asymptotic approximation does not.
- The time duration of the pulse (as measured by the length of the 1/e contour along the direction of propagation, the line at angle θ_2) is very close to that of the asymptotic approximation. However, the width (minor axis) of the numerically integrated peak is somewhat greater than that of the asymptotic approximation. Also, the contours are slightly egg-shaped with a little more width farther from the origin than closer relative to a symmetric shape. But the slope of the major and minor axes of the contours, predicted by the interaction of the factors F_b and F_a in (6), appears to be in good agreement.
- The reflected pulse, as expected, is very close to symmetric with the incident pulse. The reflected peak is at $x/\lambda_o = 50.14$ and $z/\lambda_o = -86.38$ as compared to specular values $100 \cdot \sin(\pi/6) = 50$ and $-100 * \cos(\pi/6) \approx -86.6$. The magnitude of the reflected peak computed from inverse transform is 0.1057 compared to the asymptotic approximation of 0.1069. In summary for this case, the asymptotic approximation gives a qualitatively and heuristically satisfactory explanation of the refracted and reflected waves.

Figs. 1 and 2 show that the wave in the Lorentz model medium, with $n_g = 3.735$, is moving much more slowly than the wave in free space because the transmitted contours are visibly much closer to the origin and the length to the 1/e contour is much smaller. In addition, the reflected peak shows better agreement between the asymptotic specular reflection and the numerical integration. In Fig. 2 the peaks as found from numerical integration (on a grid of $0.01\lambda_o$ by $0.01\lambda_o$) are plotted as an "x" in the center of the contours.

Fig. 3 shows details of the comparison of the Lorentz model results of Fig. 2 with a numerical integration of the case of constant $n_g = 3.7352 + 0.003\,309j$ and constant $\epsilon_{2rg} = 3.8368 +$

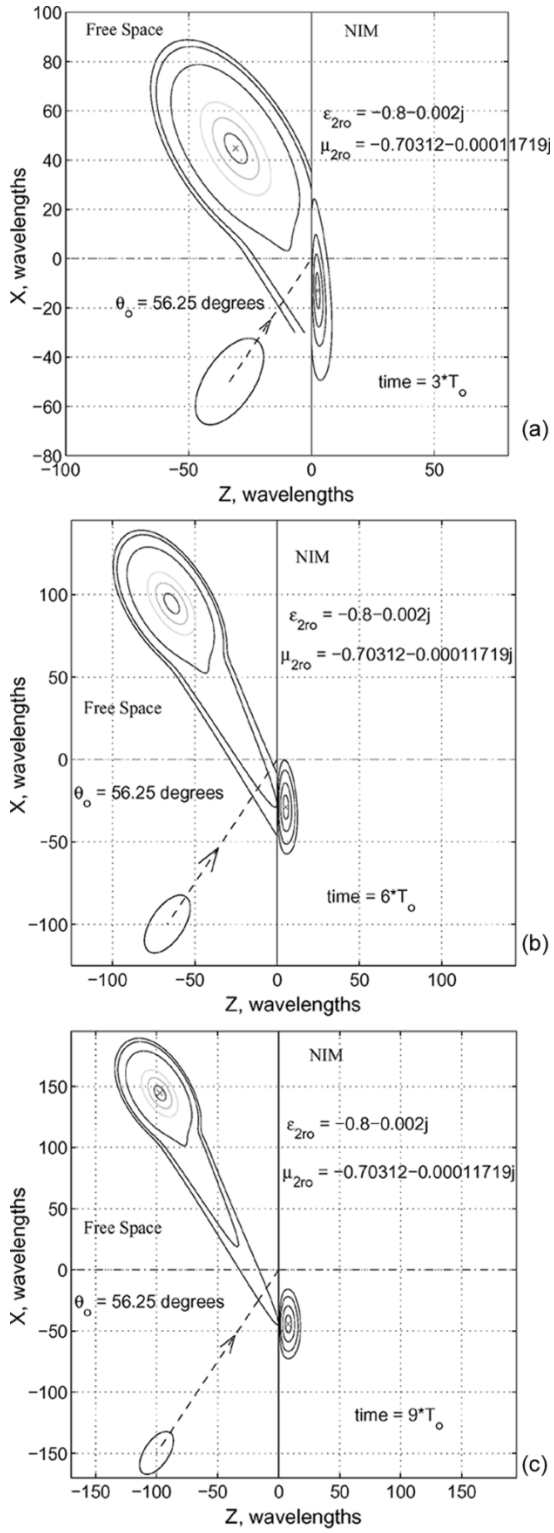

Fig. 4. Progression of the backward lateral wave in time for a Lorentz model with $n_2 = -0.75 - 0.001j$. The reflected contours are at 0.9, 0.65, 1/e, $0.1 * 1/e$, $0.02 * 1/e$, and $0.01 * 1/e$ of reflected peak. The transmitted contours are at 0.9, 0.65, 1/e, and $0.2 * 1/e$ of peak at x in the NIM. The subplots show contours of $|H|$ (a) at $\mathrm{time} = 3T_o$, (b) at $\mathrm{time} = 6T_o$ and (c) at $\mathrm{time} = 9T_o$ for reflected and transmitted waves. Heavy contours denote the 1/e levels. The incident wave (heavy contour only) is shown at time equal to the negative of that labeled on each plot. Note that the plot scale increases with time.

$0.006\,304j$, which we call a linear model. Fig. 3 presents an enlargement of the fourth quadrant region of Fig. 2, but with

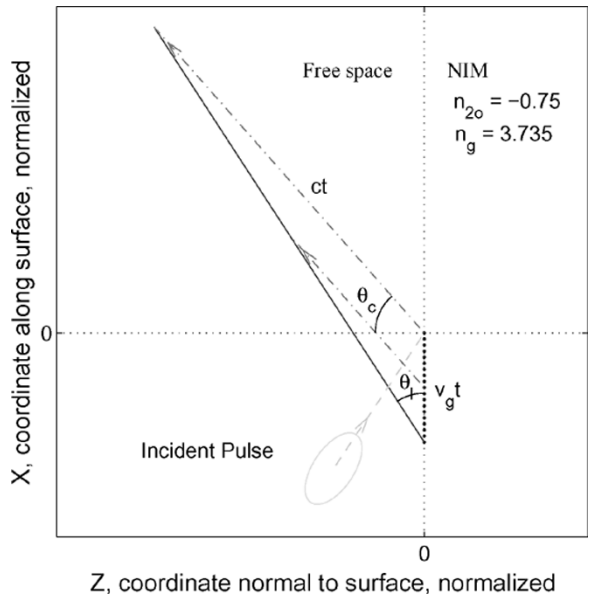

Fig. 5. Angle of the backward lateral wave. The small transmitted peak travels down the X axis and radiates at each point at the angle θ_c relative to the surface normal.

TABLE I[1]
PROGRESSION OF PEAKS IN TIME

time [1]	$3T_o$	$6T_o$	$9T_o$
$X_t\ (\lambda_o)$	-13.007	-28.885	-44.209
$Z_t\ (\lambda_o)$	2.5215	5.2335	7.923
Amplitude	0.090569	0.058165	0.042926
$X_r\ (\lambda_o)$	44.724	94.610	144.491
$Z_r\ (\lambda_o)$	-30.789	-64.019	-97.290
Amplitude	0.941092	0.918465	0.885763
BWLW contour level	0.00692	0.00676	0.00652

comparison of two numerical integration solutions. There is at least as much difference between these two numerical solutions as between the asymptotic approximation and the Lorentz model solution. The Lorentz model solution has a higher peak, by about 6%, and has more asymmetry than the linear model, but qualitatively the solutions are similar.

We have calculated reflected and transmitted waves for the case of a medium with $n_{2o} = -1.25 - 0.001j$ and with various positive values of n_g and we find similar results. The asymptotic solution provides a good qualitative understanding and prediction of the velocity of the transmitted peak and the approximate size and orientation of the 1/e contour. If $n_2 < -1$, there is no critical angle, and the asymptotic approximation given by (6) is valid for all angles of incidence.

IV. INCIDENCE BEYOND THE CRITICAL ANGLE: THE BACKWARD LATERAL WAVE AND GOOS–HANCHEN EFFECT

For two positive-index dielectric materials with a planar boundary, with incidence from a medium of larger positive index onto one of smaller index, there is a critical angle for total internal reflection. At angles slightly larger than this critical

[1]The first three rows refer to the transmitted peak, the next three refer to the reflected peak, and the last row is the approximate BWLW amplitute.

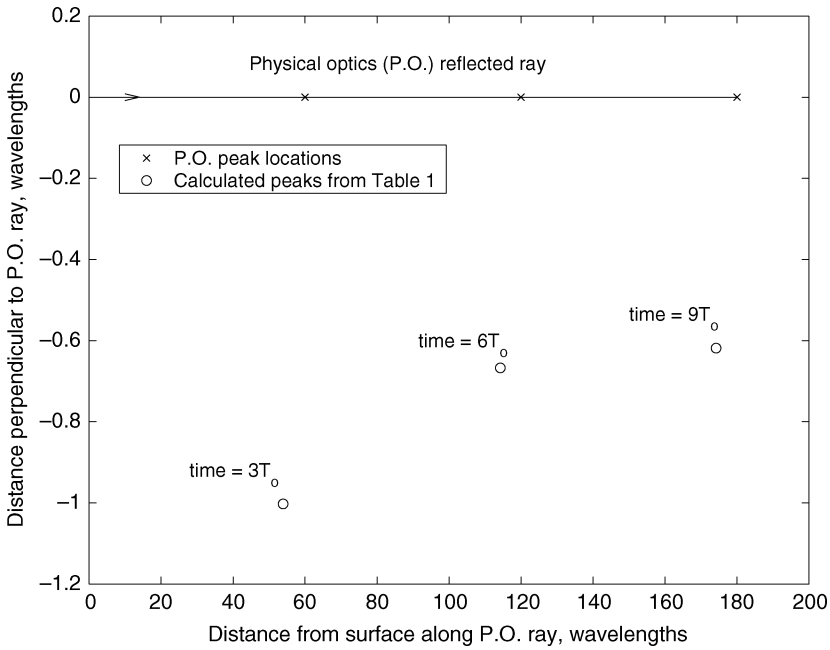

Fig. 6. Goos Hanchen shift of reflected peaks. The shift is toward the negative x direction by slightly less than a wavelength. The calculated peaks lag behind the P.O. peaks by about 5 wavelengths.

angle, there are two known, yet somewhat point of incidence of the center of the pulse.unusual, phenomena known as the lateral wave and the Goos–Hanchen shift [15]. We consider here a backward lateral wave and find numerical solutions that demonstrate this behavior for the case of incidence from free space to NIM of index between -1 and 0, specifically for $n_{2o} = -0.75 - 0.001j$ as considered in the previous section. There is a critical angle $\theta_c = \sin^{-1}(|\mathrm{Re}\{n_{2o}\}|) \approx 48.59°$. We present here results for $\theta_o = 5\pi/16$ radians $= 56.25°$. In this solution the small transmitted-wave peak moves backward along the surface (compared to the usual positive index case) and causes a small amplitude lateral wave on this backward side of the main reflected pulse. We call this the backward lateral wave (BWLW).

The lateral wave is separated from the radiated-wave term in an asymptotic expansion as the part of the complex integral contributed by the path around a branch point. When incidence is not beyond the critical angle, the branch point lies in a part of the complex plane of integration that does not come close to the steepest-descent curve and thus does not make a significant contribution. The standard theory of these asymptotic expansions is done in terms of single frequency (cw) waves. From a study of continuous waves at the interface of a normal dielectric and a NIM, we predicted the existence of backward lateral waves and other asymptotic phenomena [7]. The numerical case presented here shows the features of a backward lateral wave examined in a region fairly close to the origin, that is, the (2-D)

Fig. 4 shows contour plots of the reflected and transmitted waves (the transverse component H_y) at times $t = 3T_o$, $6T_o$ and $9T_o$, respectively, after the peak of the incident pulse (same width and duration as in previous section) arrives at the origin. To illustrate the scale, the incident 1/e contour is shown at time $= -t$. Recall that $cT_o = 20\lambda_o$, so that at $t = 3T_o$ the reflected peak is about $60\lambda_o$ from the origin, and the reflected wave has taken its elliptic shape quite accurately within 1/e of its peak. However, the outer contours are still forming in Fig. 4(a).

The asymptotic theory has a heuristic interpretation for this low-amplitude transmitted wave propagating near the surface as the source of the backward lateral wave, which shows up as the asymmetric tails in Fig. 4. The surface source point moves in the backward direction at approximately the group velocity for the dispersive NIM. Asymptotically, the BWLW radiates outwards from the surface source point at an angle to the normal equal to the critical angle. Thus, the similar triangles shown in Fig. 5 lead to the result [7] that the asymptotic BWLW will create a wave front emerging at an angle θ_l. The law of sines applied to this triangle gives, for our Lorentz case with $n = -0.75$ and $n_g = 3.735$

$$\sin^2(\theta_l) = \frac{n_g^2\left(1 - |n|^2\right)}{1 + 2n_g|n| + n_g^2}; \quad \text{thus,} \quad \theta_l \approx 33°.$$

This provides an approximate explanation of the angle of the asymmetric tails in Fig. 4, as one may read off these true-angle plots.

We compile in Table I a summary concerning the peaks in Fig. 4. The peak locations (X and Z) are given in wavelength units (taken as $c/10^{11}$ in our computations), the time is given in terms of the 1/e time duration of the Gaussian pulse ($T_o = 2 \cdot 10^{-10}$ s) and the amplitudes are all normalized to the unit incident $H = 1$ A/m. The BWLW contour is taken from a judgment of the appearance of the plots as the $0.02 * (1/\mathrm{e}) * (\mathrm{Peak})$ contour level. It is qualitatively the highest contour where the extended tail appears.

Least-mean-square linear fits to the three transmitted peak points give constant x and z components of velocity $V_x =$

$-7.7951 \cdot 10^7$ m/s and $V_z = 1.3494 \cdot 10^7$ m/s that fit the data very closely. The resulting index $n_g = c/\sqrt{V_x^2 + V_z^2} = 3.7896$ is satisfactorily close to 3.7352 with allowance for the second-order dispersion effects.

In Fig. 6 we plot the location of the points (Z_t, X_t) compared to the straight line of the ideal physical optics reflection of the center of the incident pulse. The points where the physical optics peak would be at times $t = 3T_o, 6T_o$ and $9T_o$ are denoted by an x on the straight line, and the calculated points are shown by a small circle. The vertical displacement for large t between these two positions is interpreted as the Goos–Hanchen shift of the NIM, with the shift being in the negative X direction [17], [18]. The delay involved in the shift accounts for the calculated pulse lagging behind the instantaneous physical optics points.

V. Conclusion

We have demonstrated that an asymptotic analytic first-order approximation to the calculation of transmission and reflection at a plane boundary between free space and a NIM gives a good estimate of the negative refraction that occurs. We have provided an exact calculation of the negative refraction phenomenon for a pulse in time and 2-D space. We have also calculated a case that demonstrates the phenomenon of a backward lateral wave (as predicted on general theoretical grounds [7]) and also a small negative displacement of the peak of the reflected wave that we interpret as a Goos–Hanchen shift.

The criterion for validity of the asymptotic approximation may be stated as: n_g and ϵ_{rg} must not change greatly over the band of integration. The assumed choice of a Lorentz model with $\omega_{pe}/\omega_e = 2.5$ met this criterion for our particular choice of a time pulse with 20 cycles from maximum sinusoidal peak to the sinusoidal peak with amplitude 1/e of the maximum. However, when we look at what metamaterial designers may have achieved so far, we find considerably narrower bandwidths. For example, if we try to characterize roughly the resonances found by [16], we find that the resonances would have $\omega_{pe}/\omega_e \approx 0.5$. Then, the asymptotic approximation would not work at all for our pulse. On the other hand, a more monochromatic pulse with at least 300 cycles from maximum sinusoid to the 1/e amplitude sinusoid would satisfy the condition for validity of the asymptotic approximation. This narrower-band pulse would again exhibit negative refraction with propagation at the speed given by the group index. The calculational method should go through as in our simpler case, but the number of intervals would increase and consequently the computation time, too.

An important related conclusion is that we need to find methods to make wider-band metamaterials for practical use with pulses that are not extremely narrow band. In other words we need to find a way to increase the plasma frequency relative to the resonant frequency (for both electric and magnetic Lorentz models). That statement does not have an obvious practical solution, but it has some interpretation in that the plasma frequency of a natural material is related to its electron density, whereas the resonant frequency is typically an atomic or molecular property.

References

[1] V. G. Veselago, "The electrodynamics of substances with simultaneously negative values of ϵ and μ," *Soviet Physics USPEKHI*, vol. 10, no. 4, pp. 509–514, Jan.–Feb. 1968.

[2] J. B. Pendy, A. J. Holden, D. J. Robbins, and W. J. Stewart, "Magnetism from conductors and enhanced nonlinear phenomena," *IEEE Trans. Microwave Theory Tech.*, vol. 47, no. 11, pp. 2075–2084, Nov. 1999.

[3] J. B. Pendry, "Negative refraction makes a perfect lens," *Phys. Rev. Lett.*, vol. 85, no. 18, pp. 3966–3969, Oct. 30, 2000.

[4] D. R. Smith, W. J. Padilla, D. C. Vier, S. C. Nemat-Nasser, and S. Schultz, "Composite medium with simultaneously negative permeability and permittivity," *Phys. Rev. Lett.*, vol. 84, no. 18, pp. 4184–4187, May 1, 2000.

[5] P. M. Valanju, R. M. Walser, and A. P. Valanju, "Wave refraction in negative-index media: always positive and very inhomogeneous," *Phys. Rev. Lett.*, vol. 88, no. 18, p. 187 401, May 6, 2002.

[6] R. W. Ziolkowski and E. Heyman, "Wave propagation in media having negative permittivity and permeability," *Phys. Rev. E*, vol. 64, no. 5, pp. 056 625-1–056 625-15, Nov. 2001.

[7] A. Ishimaru, J. R. Thomas, and S. Jaruwatanadilok, "Electromagnetic waves over half-space metamaterials of arbitrary permittivity and permeability," *IEEE Trans. Antennas Propag.*, vol. 53, no. 3, pp. 915–921, Mar. 2005.

[8] D. R. Smith, D. Schurig, and J. B. Pendry, "Negative refraction of modulated electromagnetic waves," *Applied Phys. Lett.*, vol. 81, no. 15, pp. 2713–2715, Oct. 7, 2002.

[9] L. Brillouin, *Wave Propagation and Group Velocity*. New York: Academic Press, 1960, pp. 121–124.

[10] M. Born and E. Wolf, *Principles of Optics: Electromagnetic Theory of Propagation, Interference and Diffraction of Light*. Cambridge, U.K.: Cambridge Univ. Press, 1989.

[11] J. B. Pendry and D. R. Smith, "Comment on 'wave refraction in negative-indes media: always positive and very inhomogeneous'," *Phys. Rev. Lett.*, vol. 90, no. 2, p. 029 703-1, Jan. 17, 2003.

[12] Z. M. Zhang and K. Park, "On the group front and group velocity in a dispersive medium upon refraction from a nondispersive medium," *ASME J. Heat Transfer*, vol. 126, no. 2, pp. 244–249, Apr. 2004.

[13] P. Drude, "Zur Electronentheorie der Metalle," *Annalen der Physik*, vol. 1, p. 566, 1900.

[14] J. A. Stratton, *Electromagnetic Theory*. New York a: McGraw-Hill, 1941, pp. 488–490.

[15] A. Ishimaru, *Electromagnetic Wave Propagation, Radiation and Scattering*. Englewood Cliffs, NJ: Prentice Hall, 1991, pp. 165–169.

[16] A. Ishimaru, S.-W. Lee, Y. Kuga, and S. Jandhyala, "Generalized constitutive relations for metamaterials based on the quasistatic Lorentz theory," *IEEE Trans. Antennas Propag.*, vol. 51, no. 10, pp. 2250–2257, Oct. 2003.

[17] A. Lakhtakia, "Positive and negative Goos-Hanchen shifts and negative phase-velocity mediums (alias left-handed materials)," *AEU-Int. J. Electron. Commun.*, vol. 58, no. 3, pp. 229–231, 2004.

[18] D.-K. Qing and G. Chen, "Goos-Hanchen shifts at the interfaces between left- and right-handed media," *Opt. Lett.*, vol. 29, no. 8, pp. 872–874, Apr. 15, 2004.

John Rhodes Thomas (M'76) received the B.S. degree in physics from the California Institute of Technology, Pasadena, in 1957 and the M.S.E.E. degree from the University of Washington, Seattle, in 1998, where he is working on his dissertation in the field of negative index media under Prof. A. Ishimaru.

He worked for The Boeing Company from 1958 until retirement in mid 1995. From 1973 to 1995, his work was devoted mostly to electromagnetic pulse hardening of aircraft and weapon systems. In 1996, he returned to graduate school at the University of Washington.

Akira Ishimaru (M'58–SM'63–F'73–LF'94) received the B.S. degree in 1951 from the University of Tokyo, Tokyo, Japan, and the Ph.D. degree in electrical engineering in 1958 from the University of Washington, Seattle.

From 1951 to 1952, he was with the Electrotechnical Laboratory, Tanashi, Tokyo, and in 1956, he was with Bell Laboratories, Holmdel, NJ. In 1958, he joined the faculty of the Department of Electrical Engineering, University of Washington, where he was a Professor of electrical engineering and an Adjunct Professor of applied mathematics. He is currently Professor Emeritus there. He has also been a Visiting Associate Professor with the University of California, Berkeley. His current research includes waves in random media, remote sensing, object detection, and imaging in clutter environment, inverse problems, millimeter wave, optical propagation and scattering in the atmosphere and the terrain, rough surface scattering, optical diffusion in tissues, and metamaterials. He is the author of *Wave Propagation and Scattering in Random Media* (NewYork: Academic, 1978; IEEE-Oxford University Press Classic re-issue, 1997) and *Electromagnetic Wave Propagation, Radiation, and Scattering* (EnglewoodCliffs, NJ: Prentice-Hall, 1991).

Dr. Ishimaru is a Fellow of the Optical Society of America, the Acoustical Society of America, and the Institute of Physics, U.K. He has served as a member-at-large of the U.S. National Committee (USNC) and was Chairman (1985–1987) of Commission B of the USNC/International Union of Radio Science. He was the recipient of the 1968 IEEE Region VI Achievement Award and the IEEE Centennial Medal in 1984. He was appointed as Boeing Martin Professor in the College of Engineering in 1993. In 1995, he was awarded the Distinguished Achievement Award from the IEEE Antennas and Propagation Society and was elected to the National Academy of Engineering in 1996. In 1998, he was awarded the Distinguished Achievement Award from the IEEE Geoscience and Remote Sensing Society. He is the recipient of the 1999 IEEE Heinrich Hertz Medal and the 1999 URSI Dellinger Gold Medal. In 2000, he received the IEEE Third Millennium Medal. He was Editor of *Radio Science* from 1979 to 1983 and Founding Editor of *Waves in Random Media*, Institute of Physics, U.K.